Eur. Phys. J. B **13**, 279–287 (2000)

THE EUROPEAN PHYSICAL JOURNAL B

EDP Sciences

Grain growth and phason-strain field in quasicrystalline Al-Li-Cu

K. Wang[1,a], P. Donnadieu[2], and P. Garoche[1]

[1] Laboratoire de Physique des Solides, CNRS/Université Paris-Sud, 91405 Orsay Cedex, France
[2] LTPCM-ENSEEG-INPG[b], Domaine Universitaire, BP 75, 38402 Saint-Martin d'Hères, France

Received 1 February 1999 and Received in final form 12 May 1999

Abstract. We report on grain growth and related structure change in single phased Al-Li-Cu quasicrystals. The icosahedral phase grains have been investigated using scanning ion microscopy and transmission electron microscopy. Regular boundaries between large grains have been observed both before and after high temperature annealing. The electron diffraction study shows that the grain growth is accompanied by a reduction of the phason-strains. The orientation relation between grains sets the 2-fold icosahedral axes parallel, and the coincidence of the planes depends on the phason strain-field. The effect of phason-strain field on these boundaries is discussed. It is proposed that the phason strain elimination can play a role in the grain growth.

PACS. 61.44.Br Quasicrystals – 61.16.-d Electron, ion, and scanning probe microscopy – 61.14.-x Electron diffraction and scattering

1 Introduction

The quasicrystalline phase of Al-Li-Cu is the first quasicrystal (QC) to have been obtained through slow cooling. The icosahedral Al-Li-Cu quasicrystal, if slowly solidified, grows in the shape of a triacontahedron [1]. However, these tiny triacontahedra are embedded in eutectic phases. The Al-Li-Cu QC phase domains are often polyquasicrystalline, and contain considerable structural defects [2] that can be described as phason-strains [3]. From this point of view, the Al-Li-Cu QC phase is a good candidate for the investigation of structural evolution of the quasicrystalline structure. With the Al-Li-Cu system, the main problem is to avoid lithium loss under heating in order to study the structural evolution without composition change. This difficulty has been overcome using a special confinement device [4]. Using this device, we succeeded in preventing the lithium evaporation and produced large-sized single-phased samples through slow cooling (from about 620 °C to room temperature) of the remelted seeds. This device also allowed us to achieve long-time annealing up to 500 hours. The effects of high temperature thermal treatment were described in detail elsewhere [4,5].

The phason strains in the samples are likely to be frozen into the QC structure during the solidification from the melt, where no long-range order pre-exists. The order propagation of the quasicrystalline structure implies at least two processes: the sample recrystallization and the elimination of the frozen phason-strains, since both the grain boundaries and the phason strains break the long-range order. In normal crystals, the recrystallization behavior is often related to phonon-strains, corresponding to non-uniform atomic position displacements that cost elastic energy. In the case of a quasicrystal of icosahedral symmetry, structure fluctuations can be characterized by three bulk translation modes, as well as three relative phase-shift modes associated with internal atomic position rearrangements. These modes are respectively described in the so-called parallel and the perpendicular spaces in a six-dimension space description, where the parallel space corresponds to the physical space. Spatially uniform displacements in both spaces leave the system's elastic energy invariant. Spatially varying displacements in the parallel (physical) space are described by the phonon strains, while that in the perpendicular space by phason-strains.

According to their symmetry features, there is or there is not coupling between the phonon and the phason strains. For an icosahedral system, the phonon strains are decomposed into two fields, transforming respectively under two lower dimensional irreducible representations of the icosahedral group, namely Γ_1 (the one-dimensional representation) and Γ_5 (the five-dimensional representation), that correspond respectively to the dilatation and the shear. The phason-strains are decomposed into two fields as well, but transforming under Γ_4 and Γ_5, that are the four- and five-dimension representations of the icosahedral group [6]. The presence of phason-strain fields breaks the icosahedral symmetry and leads to structures that belong to subgroups of the icosahedral one. For example, a Γ_4 strain field can lead to a tetrahedral structure, while a Γ_5 strain field can lead to a pentagonal

[a] e-mail: wang@lps.u-psud.fr
[b] CNRS UMR 5614

structure. A coupling between the Γ_5 phonon-strain field and the Γ_5 phason-strain field can exist, since these two fields belong to the same group representation. On the contrary, no coupling is possible between the Γ_4 phason-strain field and any of the two phonon-strain fields, as neither of these two phonon-strain fields transform under the Γ_4 representation [6].

In the case of phonon-phason strain coupling, the reduction of the phonon strains can lead to the reduction of the phason-strains. On the contrary, no interaction is possible between phonon and phason-strains, if there is no coupling between them. In this respect, the case of the Al-Li-Cu QC phase is interesting. It has been shown that the symmetry of the structure of the as-cast samples is not perfectly icosahedral, and that the deviations from the icosahedral symmetry are described by a linear phason-strain field, that is frozen into the QC structure during the phase formation. This field transforms under the Γ_4 representation of the icosahedral group [3,7]. It is therefore not coupled to the two phonon-strain fields allowed by an icosahedral system (Γ_1 and Γ_5). Consequently, the phonon behavior has no direct influence on phason strains for this phase. Therefore the Al-Li-Cu QC phase is an adequate system to study the relation between grain growth and phason strains.

In this paper we present scanning ion microscopy, X-ray and electron diffraction observations on single phased Al-Li-Cu samples, and we discuss the relation between the phason strains and the grain boundaries. Our aim will be to examine whether the phason strains play a role in the grain size increase. As we deal here with the Al-Li-Cu system, only Γ_4 phason-strain structural defects are considered in our discussion.

2 Experimental observations

The Al-Li-Cu samples, rich in QC seeds of composition Al_6Li_3Cu, have been cut in the form of cylinders 2 cm high and 1 cm in diameter. They were placed in sealed stainless steel capsules and heated up to about 620 °C to remelt the foreign eutectic phases (mainly α-Al + Al_2LiCu). Afterward, they were slowly cooled to room temperature for several days. During the slow-cooling process a temperature gradient is applied along the cylinder axis to favor the QC phase solidification at one end of the cylinder. This method allows obtaining single-phased QC samples of 1 cm in size [8]. The annealing is realized at 575 °C using the same capsules. In both cases (slow-cooling and annealing) the capsules were filled with He gas to prevent lithium loss. The gas pressure is estimated at about 45 bars at 600 °C. In the following, the samples obtained through slow cooling after remelting will be referred to as remelted ones while that subsequently annealed at 575 °C will be called annealed ones.

2.1 Scanning ion microscopy

The effects of annealing on the grain structures are studied by means of scanning ion microscopy employing a gallium liquid metal ion source. The ion beam is deflected electrostaticaly to scan the sample surface, it can be focused to reach a spatial resolution below 40 nm. The imaging is realized by collecting the secondary electrons with a detector using a scintillator-photomultiplier combination [9]. In this observation, the maximum scanning area is limited to about 130×130 μm to avoid image distortions related to the electronic device that drives the ion-beam deflectors at high voltage, and the ion current to 10 pA to reduce sample damage. The focused ion beam (FIB) scanning microscopy allows us to directly visualize grains thanks to the so called "channeling effect". The secondary-electron yield varies according to grain orientations, leading to orientation-type image contrasts that reveal the grain morphology. Because of the high sensitivity of channeling to the orientation, it is possible to have an angular resolution well below 0.1 degree. Such deviations can hardly be resolved by conventional scanning electron microscopy.

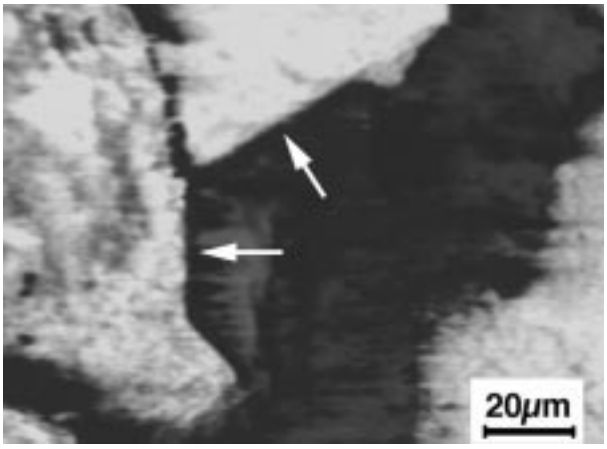

Fig. 1. The scanning ion microscopy image, built from electrons resulting from the ion impacts, taken on a single-phased Al-Li-Cu quasicrystal sample obtained by slow-cooling. Arrows indicate the regular grain boundaries.

The FIB microscopy observations are performed on single-phased Al-Li-Cu QC samples obtained by remelting and slow-cooling, and on samples subsequently annealed for a long time (10 days). In Figure 1, a FIB scanning image of the remelted sample is displayed. Here the imaging surface is a cross-section perpendicular to the sample cylinder. Figure 2 shows a scanning image of the cross-section of a cylinder sample subsequently annealed for 10 days, with the same orientation. These images display well-defined zones with different contrast levels, the result of secondary-electron yield variation. These zones reveal QC grains with different orientations relative to the ion beam direction. In fact, the secondary-electron yield reaches the minimum when the dense atomic planes in the grains are parallel to the incident ion beam. Scratch lines visible on the images are due to sample surface roughness caused by the mechanical polishing.

As far as grain morphology is concerned, straight boundaries are observed both before and after the annealing, indicating a faceting of these grains. In Figures 1

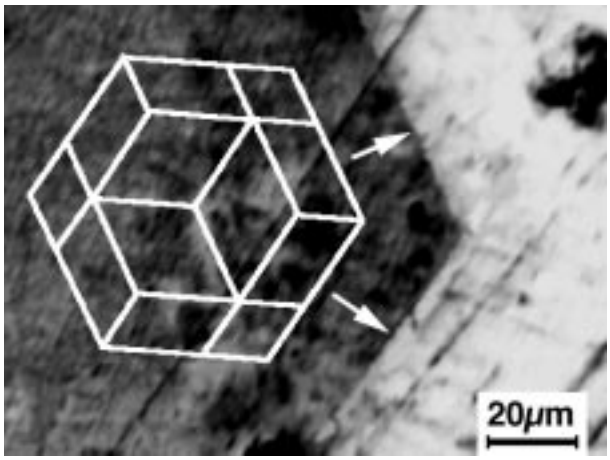

Fig. 2. The scanning ion microscopy image taken on a single-phased Al-Li-Cu quasicrystal sample after 10 days annealing. Arrows indicate the regular grain boundaries. A rhombic triacontahedron projected along a 3-fold axis is drawn in the same figure.

and 2 such boundaries are indicated by the arrows in the middle of the images. In Figure 1, two straight neighbor boundaries of about 30 μm in length separate the darkest grain from its adjacent grains. Figure 2 displays longer boundaries (exceeding 50 μm) between adjacent grains. In all the cases, the two neighbouring boundaries are well defined and form an angle of 120 ($\pm$2) degrees. We further note that only pairs of straight boundaries are observed, and the inner part of the 120-degree angle is always darker, revealing a grain in a channeling orientation [8], the secondary-electron yield being low when the angle between the incident ion beam and the atomic planes is weak.

The morphology of the channeling grains observed in Figures 1 and 2 allows us to deduce the orientation of these grains. According to the symmetry dictated morphology theory developed by Cahn and Kalonji [10], the morphology of a crystal possesses the symmetry elements that are common to the crystal and its surrounding medium. For instance, for precipitates embedded in a matrix, the morphology is dictated by the intersection group between the precipitate and the matrix point groups. In any case, the symmetry group characterizing the morphology is a subgroup of the structure point group. As the icosahedral group possesses 2-fold, 3-fold and 5-fold axes, the observation of grains with facets making 120-degree angles indicates that the grain is seen along a 3-fold axis.

The evolution of the grain sizes during annealing can also be seen through Figures 1 and 2. As shown by Figure 1, the sizes of the contrasted zones are small before annealing. This can easily be seen on the darkest channeling grain, whose size is below 100 μm. We note that there are dark grains with small size and curved boundaries in the same figure. Their low secondary-electron yield indicates that their orientation is close to the channeling grains with straight boundaries. For Figure 2, taken on an annealed sample, the image displays clearly much larger homogenous zones as compared to Figure 1. This indicates an increase of the grain sizes during the annealing that leads to grain growth. As a matter of fact, the grain sizes do not exceed, for the most part, 0.1 mm for the slow-cooled samples, while for the annealed samples they can reach 0.5 mm in the best cases [8]. More details concerning the grain size evolution can be found in reference [8].

2.2 Diffraction experiments

The Al-Li-Cu QC samples in the remelted and annealed state have been examined by means of X-ray diffraction and transmission electron microscopy. The X-ray diffraction experiments were aiming at some global information on the sample texture while the electron diffraction allows identifying the structural changes related to the grain growth due to the annealing treatment.

2.2.1 X-ray diffraction experiments

X-ray diffraction was carried out on the cylinder-shaped samples previously examined by FIB microscopy. We examined the sample surface using $\theta - 2\theta$ scans by recording the intensity of the reflection beam. Two configurations were considered. In the first case, the sample is oriented so that the reflection surface is perpendicular to the cylinder axis, *i.e.*, parallel to the surface used for FIB imaging. In the second case, a complementary orientation is used: the sample is set to have the reflection surface parallel to the cylinder axis. The experiments were carried out with a diffractometer using Co Kα radiation.

The X-ray diffraction of the remelted and annealed samples shows similar results, thus only the diagrams obtained on remelted samples are reported here. The main peaks are displayed in Figure 3 using a 6 dimensional indexation [11]. Figures 3a and 3b correspond to the two configurations described above. Obviously the diffraction diagrams in 3a and 3b are complementary to each other. The peak indexed (110001) is strong on the diffraction diagram in 3a while it is a weak peak in 3b. Since the grain size is in the 100 micron range, this effect can be interpreted by a texture showing a majority of grains with a 3-fold axis parallel to the direction used in FIB imaging. On the other hand, the strongest diffraction peak for the diagram in 3b is indexed as a (110000). This intense peak corresponds to a 2-fold icosahedral axis, which is consistent with a majority of grains having a 3-fold axis parallel to the cylinder axis.

For the remelted as well as the annealed samples, the X-ray diffraction patterns and the channeling grain morphology imaged by FIB are consistent with grains having their 3-fold axis parallel to the sample cylinder axis. As a matter of fact, it has been observed that strong channeling takes place in a quasicrystal along the major symmetry axes (2-, 3- and 5-fold axes) of the icosahedral group [12]. The above observations indicate that in our case the channeling effect occurs along a 3-fold axis of the grains for which the regular facets correspond to 2-fold planes viewed

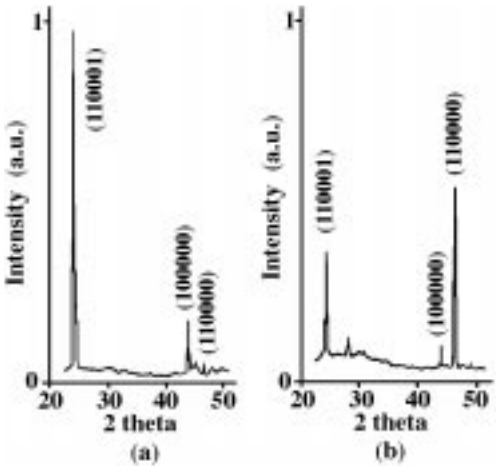

Fig. 3. Three principal diffraction peaks obtained by recording the reflections on an Al-Li-Cu remelted sample using Co Kα radiation. (a) The reflection surface is perpendicular to the sample cylinder axis; (b) the reflection surface is parallel to the sample cylinder axis.

along a 3-fold axis. Indeed, as shown in Figure 2, a triacontahedron projected along a 3-fold axis engenders a regular hexagon.

Finally, the X-ray diffraction experiments indicate that a majority of grains have a 3-fold axis parallel to the cylinder axis. As a consequence, the neighbouring zones of the grains with the dark contrast of the FIB images are very probably oriented also along a 3-fold axis, although with some misorientation. The question of the relative orientation of grains will be further examined by TEM (see Sect. 2.2.2: *Phason-strain field and grain boundaries*).

2.2.2 Electron diffraction

Electron diffraction was carried out on the remelted and annealed samples. The thin samples were taken in the cylinder samples studied by FIB, slices being cut parallel to the cylinder section. The thin samples suitable for electron microscopy were prepared by double jet polishing (for details see Ref. [13]). The electron diffraction patterns (EDPs) were recorded on Philips CM20 and Jeol 3010 electron microscopes.

Phason strains and annealing treatment

The EDPs in Figure 4 have been taken on a remelted sample, they display typical 3-fold and 5-fold symmetry patterns of icosahedral phases. It is worth noting that Figure 4a is obtained with an electron beam direction close to the ion beam one used for FIB imaging. Actually, the symmetries of the EDP in Figure 4a (resp. 4b) are only pseudo 3-fold (resp. 5 fold) symmetry. In both cases, there are deviations from the icosahedral symmetry that consist of small misalignments of the spots. For instance, it is easy to see that in the direction indicated by the arrow labeled α in 4a the diffraction spots do not form straight

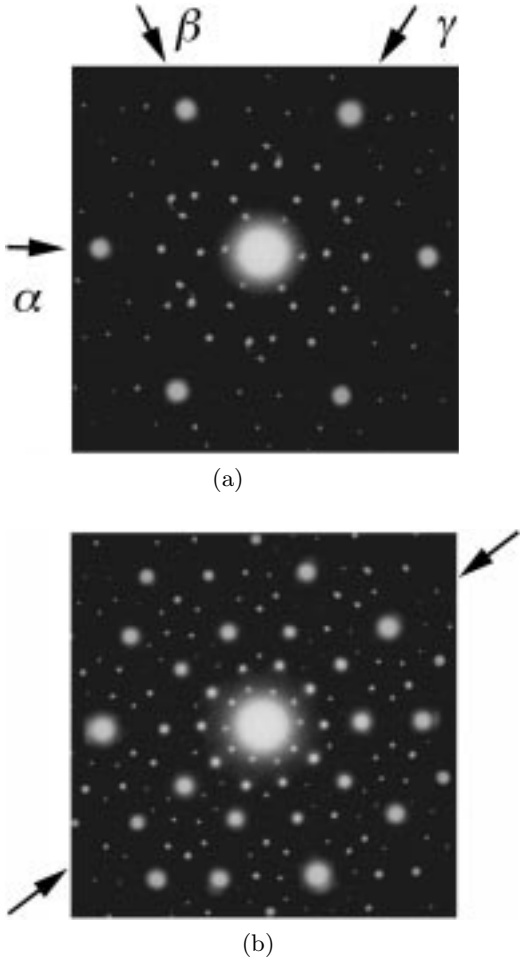

Fig. 4. Electron diffraction patterns (EDPs) taken on a remelted sample. (a) For an electron beam close to the ion beam, the EDP shows a pseudo 3-fold symmetry. The arrows labeled α and β point to the directions along which the diffraction spots form zigzag rows. Along the direction arrowed γ, the spots are aligned. (b) EDP along a 5-fold axis. Because of spot misalignment, the EDP shows only a pseudo 5-fold symmetry. The row without zigzaging is marked with two arrows.

lines. This zigzag effect is also obvious at a glancing angle. However, the three 2-fold directions imaged on the EDPs in 4a do not show equivalent distortion: the spots along the directions indicated with the arrows labeled α and β are not aligned while the direction labeled γ shows no misalignment. Similar observations can be made on the EDP in 4b: only the diffraction row marked with an arrow shows aligned spots while along the four other directions the spots zigzag.

The EDPs shown in Figure 5 correspond to the sample annealed for 10 days. Most of the remarks made for the EDPs of the remelted sample hold. We find again 3-fold symmetry axes close to the cylinder axis direction. The EDPs still show only pseudo 3-fold and 5-fold symmetry. However, a close examination is necessary to detect the deviations (along α and β in (a) and along directions other

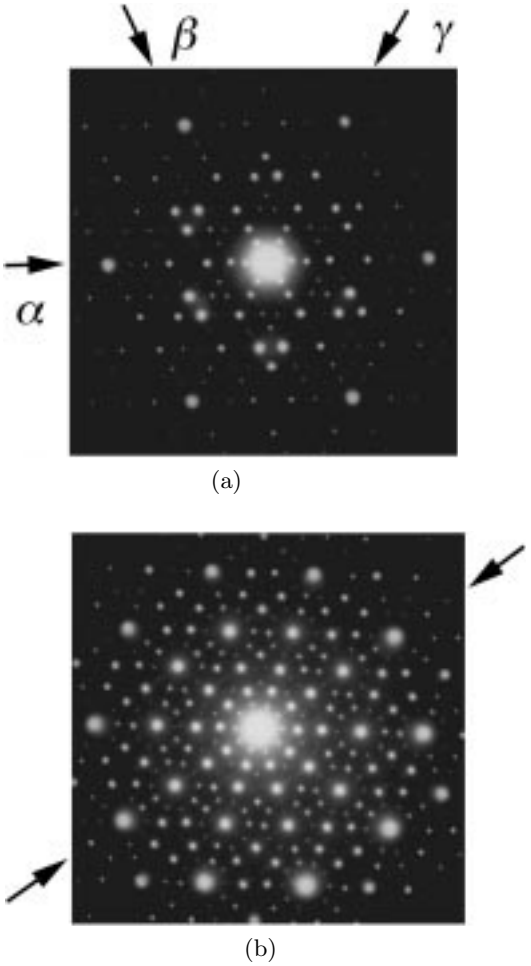

(a)

(b)

Fig. 5. Electron diffraction patterns (EDPs) taken on a sample annealed for 10 days. (a) Along a 3-fold axis, the spots show very weak misalignment (directions arrowed α and β) in comparison with Figure 4a. (b) EDP along a 5-fold axis. The spot misalignment is also reduced along the rows forming the pseudo 5-fold axis. As in 4b, the arrows indicate the row along which the spots are aligned.

than that indicated by the arrows in b). In fact they are observable only on the low intensity spots. Finally the difference between the remelted and annealed samples is a reduction of misalignment along the diffraction rows.

It is worth noting that we still observed on each of the EDPs in Figure 5 one direction without zigzag. This feature has been already described in reference [13]. Such distortion can be also described in the 6-dimensional space in terms of a phason-strain field [14,15]. The effect of a linear phason-strain field in the reciprocal space is to produce shifts of diffraction spots depending on their $Q_\perp$ components that are related to the spot intensity. The diffraction rows without misalignment are indicative of the symmetry characteristic of the strain field. Here the strain field refers to a cubic type symmetry (Ref. [13]) or more generally to a Γ_4 phason-strain field.

Therefore, as already shown in reference [3], a Γ_4 phason-strain field can account for the observed structure imperfection through electron diffraction. The annealing obviously reduces the amplitude of this phason-strain field through thermal activation. As a consequence, the annealed sample is closer to the icosahedral symmetry than the remelted sample.

Phason-strain field and grain boundaries

As reported above, EDPs allow the recognition of the presence of phason-strain fields and their evolution under annealing treatment. The point is now to investigate the influence of the phason-strain field on the coincidence of planes at grain boundaries. For simplification, we consider the remelted Al-Li-Cu phase since the phason-strain field is more pronounced in that state.

Figure 6a shows the junction between several grains in a remelted Al-Li-Cu phase, this bright field image is obtained for a tilt angle close to zero, it means that the electron beam axis is parallel to the axis of the bulk cylinder sample. The grain boundaries marked by lines in Figure 6a are not perfectly straight on a range of several micrometers but they make an average angle close to 120 degrees.

The EDPs corresponding to the grains labeled #1 #2 and #3 in Figure 6a are displayed in Figure 6b. These EDPs are obtained by a translation from grain to grain and are taken on a selected area having a 0.2 micron diameter. According to this set of EDPs, the three grains are seen along a direction close to a 3-fold axis. In fact, the grain #1 is quite well oriented along a 3-fold axis while the other two grains have a small misorientation. From the EDPs, the angle between grains can be roughly estimated to less than 0.5°. It is worth noting that the TEM image in Figure 6a is consistent with the FIB images in Figures 1 and 2, the main difference is due to the type of contrast: the channeling contrast responsible for the FIB images is more sensitive to the tilt angle than the diffraction contrast of the TEM images.

Below each EDP in Figure 6b, the directions of the 2-fold icosahedral axes are indicated by the lines labeled $A2$. It is also indicated whether there is or not shift of the spots along the 2-fold icosahedral axis. The label $A2(\|)$ means that we observe aligned spots along the 2-fold axis, the label $A2(z)$ indicates a misalignment of the spots. We precise by a superscript s when the phason-strain intensity is strong. As mentioned in the previous sections, we observe, in each grain, two diffraction rows with spot misalignment and one perfectly aligned diffraction row. It means that the grains in Figure 6 are seen along a pseudo 3-fold axis. A comparison between the EDPs #1, #2 and #3 shows that these 3 grains are oriented in a different way with respect to the phason-strain field.

According to the EDPs in Figure 6b, the relative orientation of grains sets the 2-fold axis parallel to each other. However a small rotation angle from grain to grain is difficult to detect for two reasons: the limited accuracy of the electron diffraction method and the misalignment of spots along the diffraction row. In the following, rotation of planes will be considered as negligible since it is not

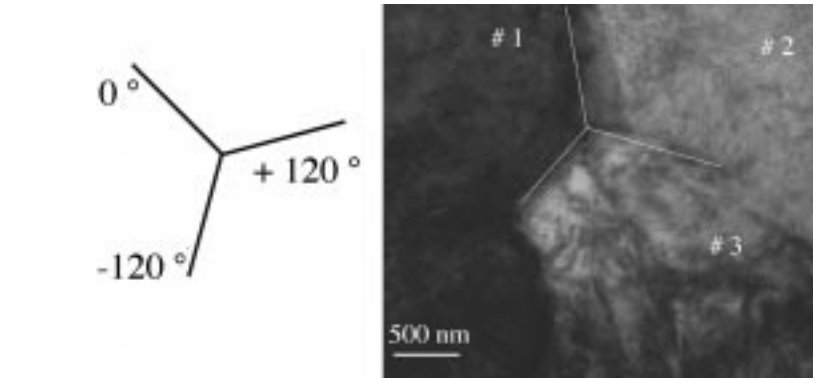

(a)

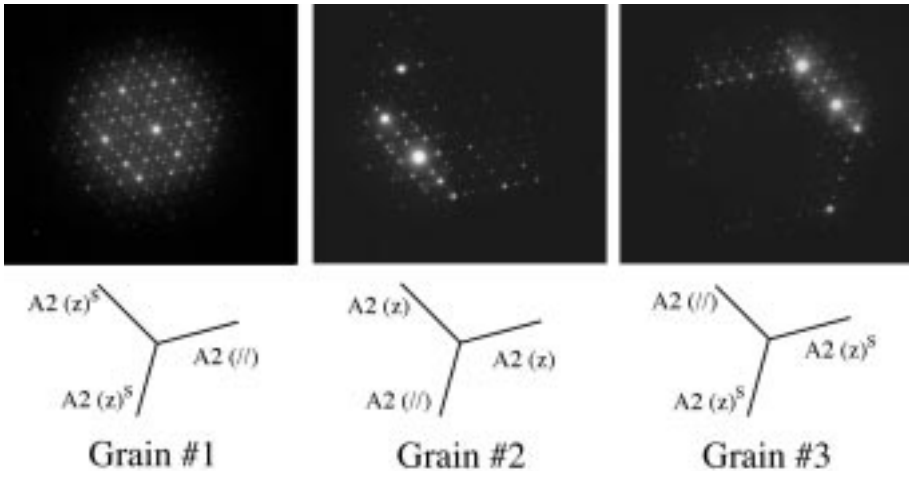

(b)

Fig. 6. (a) Bright field image showing in a remelted sample a junction between three grains labeled #1, #2 and #3. The white lines show the average position of the interface between grains. The sketch indicates the directions normal to the interfaces. (b) Electron diffraction patterns (EDPs) of the grains shown in a. The sketch below each EDP indicates by lines with $A2$ labels the direction of the 2-fold icosahedral axes. It is marked by (z) or $(\|)$ whether the diffraction row shows or not spot misalignment. The superscript s precises when the effect is strong.

obvious from the EDPs while the phason-strain field is observable on the EDPs.

Since the relative orientation between grains controls the coincidence between grain at interfaces, the possibilities of coincidence for each family of 2-fold planes can be derived; they are summarized in Table 1. The interface between the grains #1 and #2 is normal to the direction refered to as $+120°$ in Figure 6a so the directions of interest correspond to the first and the third lines in the columns #1 and #2 in Table 1. Similarly the interface between the grains #2 and #3 is normal to the direction refered to by the $-120°$ angle so the directions of interest for coincidences are the ones reported in the first two lines of the column #2 and #3 in Table 1. For both interfaces, it is clear that the status of each $A2$ direction with respect to the phason-strain field are different. So the orientation relationships of the grains sets parallel planes which correspond to a 2-fold axis modified in different manners by the phason-strain field.

Table 1. For each grain in Figure 6, the 2-fold icosahedral axes ($A2$) are refereed by the direction $0°$, $+120°$ and $-120°$ defined in Figure 6a. We indicate for each 2-fold icosahedral direction its characteristics with respect to the phason-strain field as deduced from the analysis illustrated by Figure 6b. The "$\|$" and "z" symbols hold respectively for aligned and zigzagged diffraction spots; the superscript s indicates that the phason-strain intensity is strong.

	grain #1	grain #2	grain #3
$0°$	$A2(z)^{s}$	$A2(\|)$	$A2(z)^{s}$
$+120$	$A2(z)^{s}$	$A2(z)$	$A2(\|)$
-120	$A2(\|)$	$A2(z)$	$A2(z)^{s}$

Obviously, the coincidence of the planes at the interface is dependent on the phason-strain field and, more precisely, it will depend on the magnitude and sign of the strain field. However, for a direction corresponding

to a perfectly aligned row on one side of the interface and to a misaligned row on the other side, there will be necessarily a lack of coincidence. It is worth insisting on the fact that the coincidence lost derives from the relative orientation of the pseudo 3-fold axis and that it is due to the existence of a phason-strain field.

Finally, the above observations (both microscopy and diffraction) show clearly two significant effects on the Al-Li-Cu structure, following the thermal treatment: the recrystallization and the phason-strain field elimination. In addition, TEM shows that the relative orientation of grains sets their 2-fold axis parallel. According to TEM, the phason-strain field does not have the same orientation from one grain to another. As a consequence, the presence of a phason-strain field affects the coincidence of planes at grain boundaries.

3 Phason-strain field and grain growth

The phason-strain field affects grain boundaries, and its elimination accompanies the grain growth. This raises the question as to the role played by the phason strains in the grain growth. In this section we propose a structure analysis making a connection between the phason-strain field and grain growth. We will discuss in a qualitative way how the phason-strain structure defects are related to grain boundaries, and, consequently, to grain growth.

3.1 Effect of the phason-strain field on the 2-fold planes

Here we analyze the effect of the Γ_4 phason-strain field on the grain boundaries. This will allow us to make a relation between phason-strain elimination and the grain growth. For simplicity we limit our discussion to the case of 2-fold planes, though similar arguments are hoped to be applicable to more complicated cases. As a matter of fact, there is experimental evidence that the Al-Li-Cu QC structure can be roughly described as dense atomic planes spaced in a Fibonnacci sequence along the 2-fold axes [16], in relation with the plane structures in a three-dimension Penrose tiling that can be obtained in a cut-and-projection model [17].

A Γ_4 phason-strain field in an icosahedral structure can be described by three field components that develop along three 2-fold axes that form an orthonormal set [15]. To facilitate the discussion we define these axes as along the vectors $\{|\mathrm{P}_1\rangle, |\mathrm{P}_2\rangle, |\mathrm{P}_3\rangle\}$ in Figure 7. In the presence of a Γ_4 phason-strain field, these three axes are actually the only ones among the fifteen 2-fold axes of the icosahedral group that are preserved. They form the three 2-fold axes of the tetrahedral structure. The other 2-fold axes are no longer perfect ones, and will be called pseudo axes.

As far as the ten 3-fold axes of the icosahedral symmetry are concerned, four of them are preserved (like $|\mathrm{Q}_1\rangle$ in Fig. 7) in the presence of a Γ_4 phason-strain field. The other six 3-fold axes, like $|\mathrm{Q}_2\rangle$ in the same figure, are pseudo ones as well.

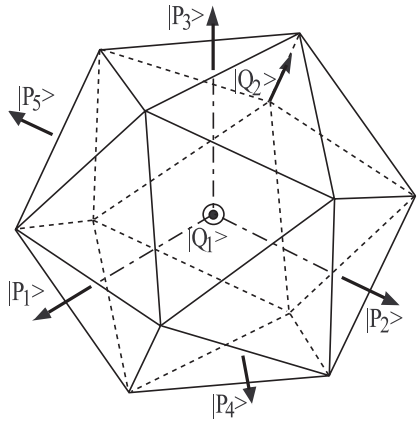

Fig. 7. In an icosahedral structure, a Γ_4 phason-strain field preserves three 2-fold axes that form an orthonormal set (defined as $\{|\mathrm{P}_1\rangle, |\mathrm{P}_2\rangle, |\mathrm{P}_3\rangle\}$ in this case). The other 2-fold axes ($|\mathrm{P}_4\rangle, |\mathrm{P}_5\rangle$,...) are pseudo ones. Consequently, $|\mathrm{Q}_1\rangle$ is a preserved 3-fold axis, while $|\mathrm{Q}_2\rangle$ is a pseudo 3-fold axis.

The effects of a linear Γ_4 phason-strain field on the 2-fold planes can be qualitatively viewed in the following way. For a 2-fold axis that is preserved by such a strain field, say $|\mathrm{P}_1\rangle$ in Figure 7, one component of this strain field increases linearly along this axis [15]:

$$\Delta W = a|\mathrm{P}_1\rangle \tag{1}$$

where ΔW describes the phason-strain field component that is defined in the perpendicular space, and a is a constant related to the strain-field magnitude. The situation here is similar to the case of the well-known one-dimensional Fibonnacci chain. The plane sequence, which is also a Fibonnacci one without the phason-stain field, is modified by the phason-strain field along this axis.

For a pseudo 2-fold axis, such as $|\mathrm{P}_4\rangle$ in Figure 7, the situation is more complicated. As a matter of fact, due to the anisotropic nature of the Γ_4 phason-strain field, its variation along this direction is not simply proportional to $|\mathrm{P}_4\rangle$. The strain field varies as a function of the other coordinates as well, and can be expressed in a general form by:

$$\Delta W = a|\mathrm{P}_4\rangle + b|\mathrm{P}_1\rangle + c|\mathrm{P}_2\rangle + d|\mathrm{P}_3\rangle \tag{2}$$

where b, c and d are constants. So besides the sequence modification like in the case of a preserved axis, the 2-fold planes along a pseudo axis are also broken following $\{|\mathrm{P}_1\rangle, |\mathrm{P}_2\rangle, |\mathrm{P}_3\rangle\}$, leading to "jags" in the plane sequence, *i.e.*, strips of planes with different sequences along this pseudo 2-fold axis.

To better illustrate the "jags", we can consider a very simple case, where a three-dimensional cubic lattice is projected onto a two-dimensional plane (x, y). We introduce an acceptance domain δ in the perpendicular space to limit the density of the projected points onto the plane, and we are interested in the lines in the (x, y) plane perpendicular to the x axis, defined by the projected points (Fig. 8). Introducing a phason-stain field that increases

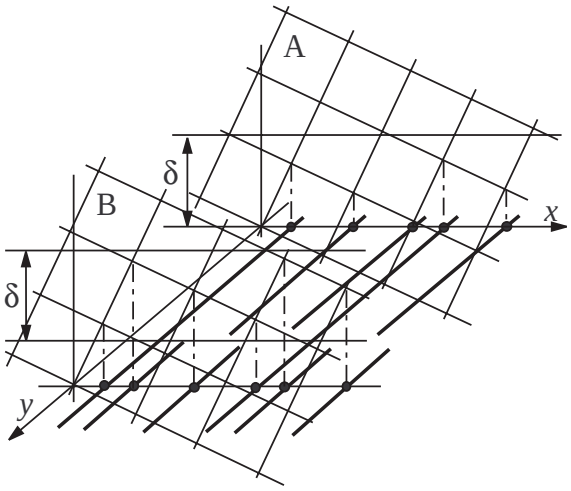

Fig. 8. The projection of a three-dimensional cubic lattice onto a two-dimensional plane (x, y), with a phason-strain field increasing along y. Points projected from the planes A and B do not fall on continuous lines perpendicular to the x axis, due to the shift of the acceptance domain δ along y. The projected points allow the definition of segments of lines following various sequences along x.

along y, so that the acceptance domain is continuously shifted along y. Considering two planes A and B of the three-dimensional lattice, points projected from these two planes do not fall on continuous lines perpendicular to the x axis in the (x, y) plane (it is easy to check that, without the shift of the acceptance domain, all projected points fall on continuous lines). So along the x axis we get segments of lines following various sequences defined by the projected points. We have a similar situation in the case of the projection from a six-dimensional space to a three-dimensional one by replacing lines by planes: the segments will correspond to jags.

3.2 Phason-strain elimination and grain growth

As we mentioned in Section 2.2.2, according to the electron diffraction (Figs. 4a and 5a), as well as to the TEM (Fig. 6), the 3-fold axis along which the ion channeling occurs is a pseudo one due to the strain field. Among the three 2-fold axes perpendicular to this pseudo 3-fold axis, only one is perfect, the other two are both pseudo axes. This situation can be illustrated by the relation between $|Q_2\rangle$, $|P_1\rangle$, $|P_4\rangle$ and $|P_5\rangle$ in Figure 7, where, perpendicular to the pseudo 3-fold axis along $|Q_2\rangle$, the 2-fold axis along $|P_1\rangle$ is perfect, while the other two axes, along $|P_4\rangle$ and $|P_5\rangle$, are pseudo ones.

Thus, the three families of 2-fold planes, parallel to the pseudo 3-fold axis (let it be $|Q_2\rangle$ in our case) and forming a $2\pi/3$ angle between them, all have their plan sequences modified along their respective 2-fold axes ($|P_1\rangle$, $|P_4\rangle$ and $|P_5\rangle$). Moreover, the two plane families along $|P_4\rangle$ and $|P_5\rangle$ undergo "jags" as well. This explains the EDPs in Figures 4a and 5a, where the three rows correspond to these 2-fold plane families. The distortion leads to a zigzag effect in two directions (along the two arrows labeled α and β), while in the last direction (labeled γ) the spots only shift along the rows.

Therefore, the phason defects of the 2-fold planes, forming the hexagon for a channeling grain (in Fig. 2), are all characterized by structure modulation along the 2-fold axes. When the neighbouring grains have their almost parallel 2-fold axes as shown in Figure 6, according to the orientation of the phason-strain field in these grains, the interface between them can be formed upon plans with modified sequences on both sides or with jagged plans on one side, or even with jagged plans on both sides. In any case, the grain interface is phason strained due to the faulted plan sequences.

The phason-strains are frozen into the QC structure during the phase formation. In the stage of the slow-solidification (before annealing), grain interfaces are thus formed upon domain structures where the phason-strain intensity is strong. During annealing, the phason-strain density is reduced all over the grain bulk. This can be seen from the electron diffraction where spot shifts are strongly reduced, as indicated by Figures 4 and 5 (see also Ref. [4]). This process will leave the grain interface unstable. A phason-strain field leads to two kinds of imperfections for an interface between two phason-strained grains: phason-strains in the 2-fold planes and phason-strains that modify the 2-fold plane sequences. The latter involve more than one atomic layer. In fact, the plane-sequence modifications in the bulk due to the phason-strain field imply, if the three-dimension lattice is decorated with atoms, rearrangements of the differently decorated 2-fold atomic planes or strips of these planes. The elimination of these phason-strains (modifying the plane sequence along the 2-fold axes) introduces density modifications in the vicinity of the interface by reducing the structure modulations through atomic diffusion, because for the Al-Li-Cu QC phase the 2-fold planes do not have the same atomic density [16]. So, upon phason-strain elimination, planar modulations near the boundary can act as local deformations by modifying interface density, at the expense of the elastic energy. Boundary displacement can thus occur. The status of coincidence between grains at their interface should then play a role in the displacement. Besides, grains with 2-fold facet planes may grow up at the expense of their neighbouring grains, if the latter's facet is not a 2-fold one, since the 2-fold planes, being the densest, have the highest cohesive energy.

The recrystallization process is very slow in Al-Li-Cu QC samples. Indeed, up to 10 days of annealing are needed to observe significant effects. This can be related to several factors. On one hand, as pointed out above, the Γ_4 phason-strain field is not coupled to phonon-modes [6]. It would thus be difficult to affect such a strain field through heating. On the other hand, the Γ_4 phason-strain field does not cost much electronic cohesive energy in Al-Li-Cu QC phase [7] and the Hume-Rothery mechanism would have little effect on it. Moreover, phason strains in adjacent 2-fold planes lead to a network of defects, which may

need a long time to relax due to correlation between them. Finally, it should be pointed out that such a "phason-strain-elimination assisted" boundary displacement will stop once the phason strains are eliminated and a stable interface is formed. Further, this is not the sole mechanism for the QC grain growth, phonon strains can always play a role. However, the phason-strain elimination seems to be a specific feature of the QC structure evolution, especially when there is no coupling between phonon and phason strains, as in the present case.

4 Conclusion

Regular grain boundaries are observed in single-phased Al-Li-Cu samples by using focused ion beam scanning microscopy. These boundaries can be identified as 2-fold planes for channeling grains. High temperature annealing of the samples leads to grain growth as well as the elimination of the Γ_4 phason-strain field, as shown by electron diffraction study. Transmission electron microscopy shows that the grains' orientation relationships set their 2-fold axes parallel from grain to grain. However, the phason-strain field is distributed in a different way from one grain to its neighbour. A consequence is that the coincidence between grains at the interfaces will be related to the phason strain field intensity. The modulations of the 2-fold planes in an icosahedral structure due to the Γ_4 phason-strain field are discussed. The results are analyzed in terms of destabilization of the 2-fold grain boundaries by the phason-strain elimination process, leading to grain growth through boundary displacements.

The authors thank Dr. Y. Calvayrac from CECM/CNRS (Vitry, France) for X-ray diffraction experiments.

References

1. B. Dubost, J.M. Lang, M. Tanaka, P. Saintfort, M. Audier, Nature **324**, 48 (1986).
2. P.A. Heiney, P.A. Bancel, P.M. Horn, J.L. Jordan, S. LaPlaca, J. Angilello, F.W. Gayle, Science **238**, 660 (1987).
3. Z.H. Mai, S.Z. Tao, L.Z. Zeng, B.S. Zhang, Phys. Rev. B **38**, 12913 (1988); F.H. Li, G.Z. Pan, S.Z. Tao, M.J. Hui, Z.H. Mai, X.S. Chen, L.Y. Cai, Philos. Mag. B **59**, 535 (1989).
4. P. Donnadieu, K. Wang, C. Degand, P. Garoche, J. Non-Cryst. Sol. **183**, 100 (1995).
5. C. Degand, K. Wang, P. Garoche, J. Non-Cryst. Sol. **153** & **154**, 478 (1993).
6. P. Bak, Phys. Rev. B **32**, 5764 (1985).
7. K. Wang, P. Garoche, Phys. Rev. B **55**, 250 (1997).
8. K. Wang, P. Garoche, L. Dumoulin, J. Phys. Cond. Matter **10**, 3479 (1998).
9. K. Wang, H.B. Yin, N. Karkour, D. Linget, F. Pesty, L. Dumoulin, P. Garoche (to be published in Scanning Microscopy).
10. J.W. Cahn, G. Kalonji, in *Proc. of the Int. Conf. on Solid-Solid Phase Transformations*, edited by H.I. Aaronson, R.F. Sekerka, D.E. Laughlin, C.M. Wayman (The Metallurgical Society of AIME, Pittsburg, 1982), Vol. 1, p. 3.
11. P.A. Bancel, P.A. Heiney, P.W. Stephens, A.I. Goldman, P.M. Horn, Phys. Rev. Lett. **54**, 2422 (1985).
12. E.H. du Marchie van Voorthuysen, P.J.M. Smulders, R.D. Werkman, J.L. de Boer, S. van Smaalen, Phys. Rev. B **45**, 9667 (1992).
13. P. Donnadieu, J. Phys. I France **4**, 791 (1994).
14. T.C. Lubensky, J.E.S. Socolar, P.J. Steinhardt, P.A. Bancel, P.A. Heiney, Phys. Rev. Lett. **57**, 1440 (1986).
15. Y. Ishii, Phys. Rev. B **39**, 11862 (1989).
16. M. de Boissieu, C. Janot, L.M. Dubois, M. Audier, B. Dubost, J. Phys. Cond. Matter **3**, 1 (1991).
17. M. Duneau, A. Katz, Phys. Rev. Lett. **54**, 2688 (1988).
18. R. Lück, in *Quasicrystalline Materials*, edited by Ch. Janot, J.M. Dubois (World Scientific, Singapore, 1988), p. 308.